On the Structure of the Iron K Edge

P. Palmeri[1], C. Mendoza[2], T. R. Kallman,

NASA Goddard Space Flight Center, Greenbelt, MD 20771

and

M. A. Bautista

Centro de Física, IVIC, Caracas 1020A, Venezuela

ABSTRACT

It is shown that the commonly held view of sharp Fe K edges must be modified if the decay pathways of the resonances converging to the K thresholds are adequately taken into account. These resonances display damped Lorentzian profiles of nearly constant widths along the spectroscopic series that are smeared to impose continuity across the threshold. By modeling the effects of K damping on opacities, it is found that the broadening of the K edge grows with the ionization level of the plasma, and the appearance at high ionization of a localized absorption feature around 7.2 keV is identified as the Kβ unresolved transition array.

Subject headings: atomic processes—line: formation—line: profiles—X-rays: general

1. Introduction

Absorption and emission features arising from iron K-shell processes are observed in the majority of X-ray spectra, and are therefore of practical importance in high-energy astrophysics. This is primarily due to the iron cosmic abundance, but also to the relatively unconfused spectral region where they appear. Although the observational technology in X-ray astronomy is still evolving, many of these features are being resolved and exploited as

[1]Research Associate, Department of Astronomy, University of Maryland, College Park, MD 20742

[2]Permanent address: Centro de Física, IVIC, Caracas 1020A

plasma diagnostics. In this respect, they are naturally grouped according to their origin, i.e. bound–bound or bound–free ionic transitions, and much of the interpretation of the latter has relied on atomic calculations (Verner & Yakovlev 1995; Berrington et al. 1997; Donnelly et al. 2000; Berrington & Ballance 2001) that predict a sharp increase of the photoabsorption cross section at the K-shell threshold. The purpose of this communication is to emphasize that this commonly held view is incorrect due to an oversimplified treatment of the decay pathways of the resonances converging to this limit, and that previous astrophysical inferences from K-edge structures should thus be revised.

2. Constancy of K damping

When a photon is sufficiently energetic to promote a K-shell electron to an excited Rydberg state, the latter decays through both radiative and autoionization (Auger) transitions. Illustrating these processes in the relatively simple case of Ne-like Fe XVII, the photoexcited K-vacancy states

$$h\nu + 1\mathrm{s}^2 2\mathrm{s}^2 2\mathrm{p}^6 \longrightarrow 1\mathrm{s}2\mathrm{s}^2 2\mathrm{p}^6 n\mathrm{p} \tag{1}$$

have access to a decay tree that can be outlined as follows:

$$1\mathrm{s}2\mathrm{s}^2 2\mathrm{p}^6 n\mathrm{p} \xrightarrow{\mathrm{K}n} 1\mathrm{s}^2 2\mathrm{s}^2 2\mathrm{p}^6 + h\nu_n \tag{2}$$

$$\xrightarrow{\mathrm{K}\alpha} 1\mathrm{s}^2 2\mathrm{s}^2 2\mathrm{p}^5 n\mathrm{p} + h\nu_\alpha \tag{3}$$

$$\xrightarrow{\mathrm{KL}n} \begin{cases} 1\mathrm{s}^2 2\mathrm{s}^2 2\mathrm{p}^5 + e^- \\ 1\mathrm{s}^2 2\mathrm{s} 2\mathrm{p}^6 + e^- \end{cases} \tag{4}$$

$$\xrightarrow{\mathrm{KLL}} \begin{cases} 1\mathrm{s}^2 2\mathrm{s}^2 2\mathrm{p}^4 n\mathrm{p} + e^- \\ 1\mathrm{s}^2 2\mathrm{s} 2\mathrm{p}^5 n\mathrm{p} + e^- \\ 1\mathrm{s}^2 2\mathrm{p}^6 n\mathrm{p} + e^- \ . \end{cases} \tag{5}$$

The radiative branches are controlled, as indicated in Eqs. (2–3), by the Kα (2p $\rightarrow$ 1s) array at $\sim \lambda 1.93$ Å and the Kn (np $\rightarrow$ 1s) of which the most salient is the K$\beta \equiv$ K3 array at $\sim \lambda 1.72$ Å. Mendoza et al. (2002) have recently demonstrated that, for any K-vacancy fine-structure state in the Fe isonuclear sequence, the width ratio $\Gamma(\beta) : \Gamma(\alpha) \lesssim 0.23$.

Equation (4) contains the participator Auger (KLn) channels where the np outer electron is directly involved in the decay. By contrast, in the KLL channels (Eq. 5) the np Rydberg electron remains a spectator. It has also been demonstrated by Mendoza et al. (2002) that, for any Fe K-vacancy fine-structure state with a filled L shell, the total Kα

and KLL widths are practically independent of both the principal quantum number $n \geq 3$ of the outer-electron configuration and the electron occupancy $N > 9$, and keep a ratio of $\Gamma(\mathrm{KLL}) : \Gamma(\alpha) \sim 1.5$. These findings illustrate the application of Gauss's law at the atomic scale as previously discussed by Manson et al. (1991) in the context of the inner-shell properties of Kr and Sn. Small quantum-mechanical deviations may occur via shake processes caused by strong admixture of levels with different outer-electron configurations; for Fe ions with $10 \leq N \leq 17$, for instance, the variations in the Kα widths by such processes have been estimated to be less than 5%. Furthermore, Mendoza et al. have also determined that Auger decay is 94% dominated by the KLL channels in Fe XVII and by no less than 76% in Fe X. Furthermore, preliminary calculations for other members of the Fe isonuclear sequence with $N > 17$ indicate that the KLL branching ratio is not significantly reduced even though the stronger of the KLM and KMM branches become spectator processes. Since both the participator Kn and KLn widths decrease with the effective quantum number as $\sim (n^*)^{-3}$, the total widths of K-vacancy states within an ionic species may be assumed constant for $n \to \infty$; for members with a filled L shell, they are also to a good approximation independent of N. In line with the previous discussions by Gorczyca (2000) and Gorczyca & McLaughlin (2000), the width constancy of high-n K resonances imprints distinctive signatures on the threshold structures of the photoabsorption cross sections that have been actually measured in the laboratory in O I and Ne I, but which have been seriously underestimated in many atomic calculations.

3. The Fe XVII case

Traditional scattering approaches may present difficulties in treating the effects of spectator Auger decay. For instance, the Breit–Pauli R-matrix (BPRM) method (Berrington et al. 1978) is based on the close-coupling approximation whereby the wavefunctions for states of an N-electron target plus a colliding electron are expanded in terms of a finite number of target eigenfunctions. As can be deduced from Eq. (5), BPRM calculations can handle spectator Auger channels only for low-n K resonances since the close-coupling expansion must explicitly include nl target states. However, Gorczyca & Robicheaux (1999) have modified BPRM to implicitly account for the spectator Auger channels by means of an optical potential devised from multichannel quantum defect theory. A target-state energy now acquires the imaginary component

$$E_k \to E_k - \mathrm{i}\Gamma_k/2 \tag{6}$$

where Γ_k is its partial decay width. This treatment of spectator Auger decay is thus analogous to that of radiation damping (Robicheaux et al. 1995).

In order to discern the contributions of the KLL channels to the total Auger widths, several BPRM calculations are carried out for the $Fe^{17+}+e^-$ system. Firstly, only target levels from the $1s^22s^22p^5$, $1s^22s2p^6$, and $1s2s^22p^6$ configurations are included in the expansion thus only accounting for participator Auger decay. In a second calculation, levels from the $1s^22s^22p^4n$p, $1s^22s2p^5n$p, $1s^22p^6n$p configurations with $n \leq 4$ are added to the target representation which now maps out the complete Auger manifold for the $1s^{-1}3$p and $1s^{-1}4$p resonances. In Table 1, the resulting Auger widths for these resonances are compared; increases by KLL decay greater than an order of magnitude and constant total Auger widths can be seen.

In a further calculation, the BPRM plus optical potential approach of Gorczyca & Robicheaux (1999) is employed to study the effects of radiation and Auger damping on the resonance structure. Fig. 1 shows the photoabsorption cross section of the $1s^22s^22p^6\ ^2S_{1/2}$ ground state of Fe XVII in the near K-threshold region. It may be seen that the undamped cross section is populated by a double series ($1s^{-1}n$p $^{3,1}P^o_1$) of narrow and asymmetric resonances that converge to a sharp K edge. The inclusion of radiation (Kα) and Auger (KLL) dampings leads to resonance series with constant widths and symmetric profiles that get progressively smeared with increasing n to produce a smooth transition through the K threshold; in low resolution, the edge would then appear to be downshifted in energy. The symmetric Auger profiles are, as discussed by Nayandin et al. (2001), a consequence of the fact that KLL channels give rise to continuum states that can only be reached by dipole forbidden direct photoionization of the ground state, and thus cause the Fano q parameter to tend to infinity. With respect to radiation damping, the dominance of the Kα over the Auger participator channels causes the modified Fano q parameter (Robicheaux et al. 1995) to be large so as to also yield a symmetric profile. Resonance smearing is the result of oscillator strength conservation which must enforce an approximate $(n^*)^{-3}$ reduction of the resonance peak-value because of the constant widths.

3.1. K-edge spectral signatures

An advantage of the simple behavior of K damping is that its impact on opacities can be estimated by means of an analytic model. The latter has been constructed and validated with the BPRM photoabsorption cross section of Fe XVII: the damped $1s^{-1}3$p resonances are fitted with Lorentzian profiles and extrapolated with n^* assuming constant widths and intensities decreasing with $(n^*)^{-3}$, the resonance positions being deduced by the usual Ritz formula. The cross sections of all the other Fe ions in the near threshold region are then determined in a similar fashion assuming a single $1s \rightarrow n$p Rydberg series of Lorentzian resonances for each species with $n \geq 2$ for $4 \leq N \leq 9$, $n \geq 3$ for $10 \leq N \leq 17$, and $n \geq 4$ for $18 \leq N \leq 26$. Since the resonance widths can be assumed constant in systems with $N > 9$ (Mendoza et al. 2002), they are assigned the value of the 3p resonances in Fe XVII, namely 4.5×10^{-2} Ryd. For $N \leq 9$, this value is scaled by a factor of $N(N-1)/90$. The resonance intensities of the first few members of each series are obtained from multiplet f-values computed with the atomic structure code HFR (Cowan 1981), and the K-threshold positions and background cross sections are taken from Verner & Yakovlev (1995).

The monochromatic opacities are generated with the XSTAR program (Kallman & Bautista 2001); the self-consistent ionization balance and electron temperature are computed under the assumption that ionization and heating are primarily due to an external source of continuum photons and that all processes are in a steady state. Solar abundances and a $F_\epsilon \sim \epsilon^{-1}$ continuum power law are adopted. As shown in Fig. 2, results are characterized in terms of the familiar ionization parameter $\xi \equiv L/nR^2$ in the range $0.01 \leq \xi \leq 100$ where L is the luminosity of the incident X-ray radiation, n the gas density, and R the distance from the radiation source. Two distinctive spectral signatures emerge: (i) the concept of a sharp edge only applies for low ionization plasmas ($\log \xi \sim -2$) and its progressive broadening is a function of ionization; (ii) for $\log \xi \gtrsim 0$, a strong absorption feature appears at the piedmont (~ 7.2 keV) caused by the Kβ unresolved transition array (UTA).

The features produced by the smeared resonances on the K-edge opacities really stand out in a comparison with opacities computed with undamped photoabsorption cross sections. The latter can be approximated by replacing the Lorentzian profiles with the Fano type with constant asymmetry parameters $q = 200$, i.e. the undamped value for the 3p resonance in Fe XVII. The undamped widths are obtained with HFR for the first member of each series and scaled down by $(n^*)^{-3}$ for the higher. The resonant cross section is deduced from the following approximate formula:

$$q^2 \approx \frac{2f(g,r)}{\pi \Gamma f(g,c)} \tag{7}$$

where $f(g,r)$, calculated with HFR, is the oscillator strength for the transition between the ground state and the non-interacting resonance, Γ is the resonance width, and $f(g,c)$ is the oscillator strength for the transition between the ground and the continuum states and is proportional to the resonant cross section. A comparison between damped and undamped opacities at $\xi = 10$ is shown in Fig. 3 where the steady upclimb in the former is replaced by sharp steps in the latter. Moreover, the role of resonances in the damped case, in particular the Kβ UTA, becomes more dominant.

4. Discussion

Broad K-edge absorption structures have been widely observed in the X-ray spectra of active galactic nuclei and black-hole candidates as reviewed by Ebisawa et al. (1994) and more recently reported by Done & Zycki (1999) and Miller et al. (2002). They have been interpreted in terms of the reflection of X-rays by optically thick accretion disks around central compact objects, partial absorption models, and relativistic broadening. Furthermore, an unidentified local absorption feature at ~ 7 keV just below a smeared K edge has been reported by Ebisawa et al. (1994) in the bright GS 1124–68 X-ray nova and by Pounds & Reeves (2002) in the MCG-6-30-15 Seyfert 1 galaxy; in this respect, the fitted ionization parameter ($\xi \sim 5.9$) in the latter seems to support our predicted edge signatures. It is expected that the present findings will contribute to a more realistic spectral modeling above 7 keV which has recently been described as critical by Pounds & Reeves (2002). However, quantitative modeling implies a systematic revision of the inner-shell photoionization cross sections for the Fe isonuclear sequence which is currently underway.

We are indebted to an anonymous referee for suggestions that have improved the presentation of the material in this report. CM acknowledges a Senior Research Associateship from the National Research Council. MAB acknowledges partial support from FONACIT, Venezuela, under Proyect No. S1-20011000912.

REFERENCES

Berrington, K.A., Ballance, C. 2001, J. Phys. B 34, 2697

Berrington, K.A., Burke, P.G., Le Dourneuf, M., et al. 1978, Comput. Phys. Commun. 14, 367

Berrington, K., Quigley, L., Zhang, H.L. 1997, J. Phys. B 30, 5409

Cowan, R.D. 1981, The Theory of Atomic Structure and Spectra (Berkeley, USA: University of California Press)

Done, C., Zycki, P.T. 1999, MNRAS 305, 457

Donnelly, D.W., Bell, K.L., Scott, M.P., Keenan, F.P. 2000, ApJ 531, 1168

Ebisawa, K., Ogawa, M., Aoki, T., et al. 1994, PASJ 46, 375

Gorczyca, T.W., Robicheaux, F. 1999, Phys. Rev. A 60, 1216

Gorczyca, T.W. 2000, Phys. Rev. A 61, 024702

Gorczyca, T.W., McLaughlin, B.M. 2000, J. Phys. B 33, L859

Kallman, T., Bautista, M. 2001, ApJS 133, 221

Manson, S.T., Theodosiou, C.E., Inokuti, M. 1991, Phys. Rev. A 43, 4688

Mendoza, C., Palmeri, P., Kallman, T.R., Bautista, M. 2002, to be published

Miller, J.M., Fabian, A.C. , Wijnands, R., et al. 2002, ApJ, in press

Nayandin, O., Gorczyca, T.W., Wills, A.A., et al. 2001, Phys. Rev. A 64, 022505

Pounds, K.A., Reeves, J.N. 2002, preprint (astro-ph 0201436)

Robicheaux, F., Gorczyca, T.W., Pindzola, M.S., et al. 1995, Phys. Rev. A 52, 1319

Verner, D.A., Yakovlev, D.G. 1995, A&AS 109, 125

This preprint was prepared with the AAS LATEX macros v5.0.

Table 1. Auger widths for the $1s^{-1}np$ resonances in Fe XVII

State	E (eV)	$\Gamma(\mathrm{KL}n)^{a}$ (eV)	$\Gamma(\mathrm{KL}n+\mathrm{KLL})^{b}$ (eV)
$1s^{-1}3p\ ^3P^o_1$	7.187	3.80×10^{-2}	6.50×10^{-1}
$1s^{-1}3p\ ^1P^o_1$	7.192	2.17×10^{-2}	6.34×10^{-1}
$1s^{-1}4p\ ^3P^o_1$	7.422	1.39×10^{-2}	6.15×10^{-1}
$1s^{-1}4p\ ^1P^o_1$	7.425	7.95×10^{-3}	6.08×10^{-1}

[a]Includes only participator (KLn) Auger channels

[b]Includes both participator (KLn) and spectator (KLL) Auger channels

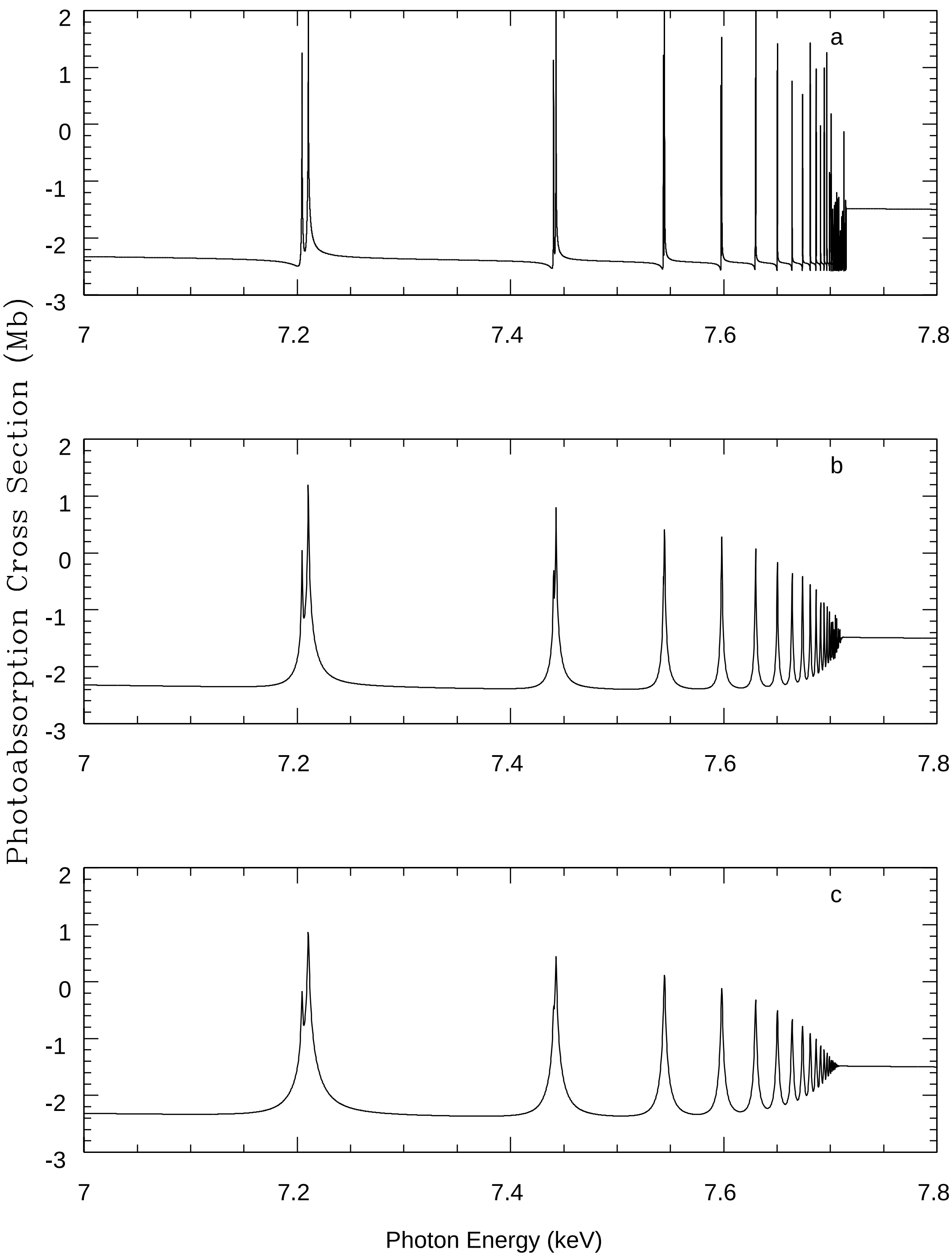

Fig. 1.— Total photoabsorption cross section of Fe XVII computed with the BPRM method (a) without damping, (b) with radiation damping, and (c) with both radiation and spectator Auger damping.

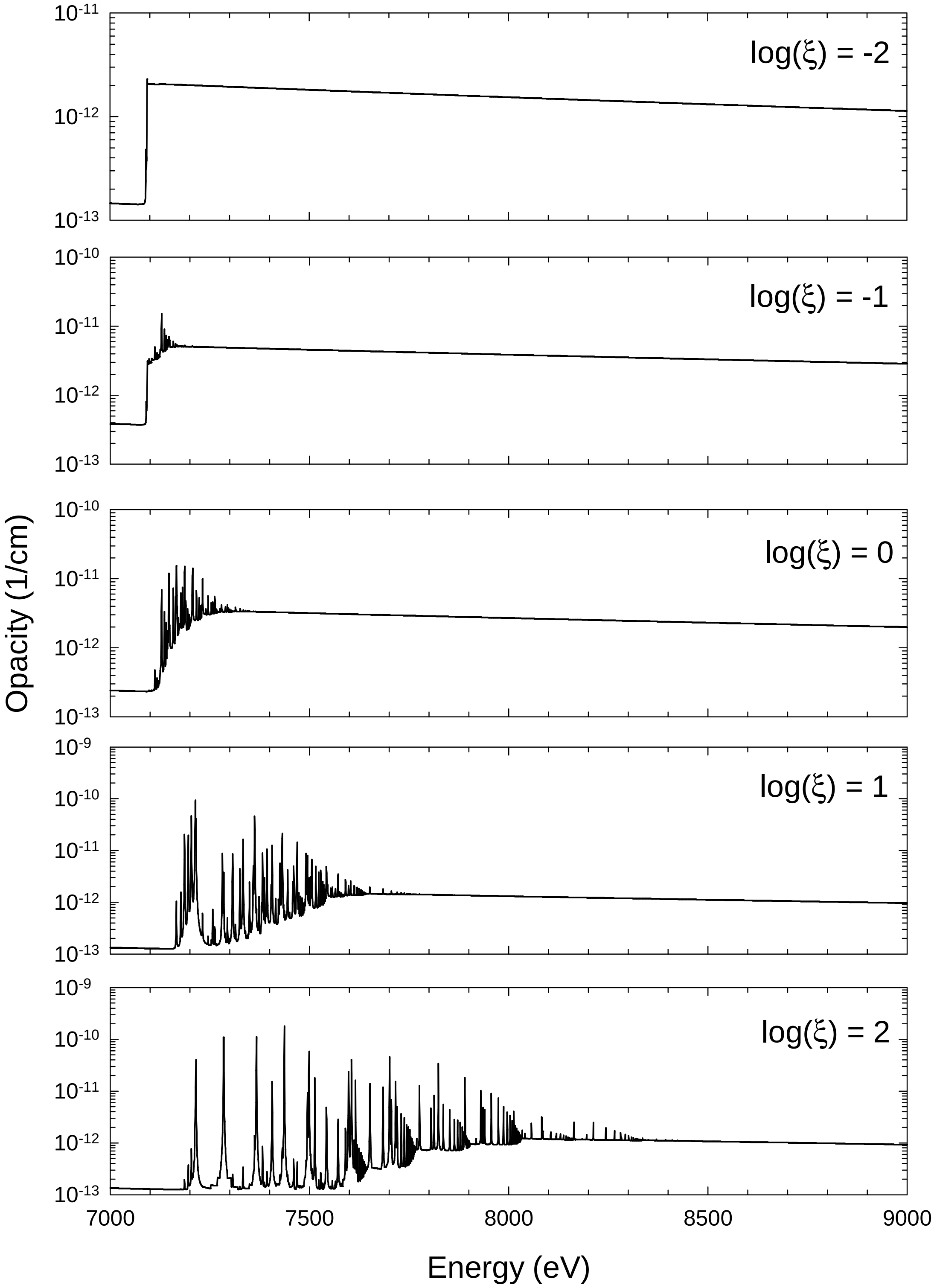

Fig. 2.— Opacities for a photoionized gas with solar elemental abundances as a function of photon energy in the region of the iron K edge. Plots correspond to different values of the ionization parameter ξ.

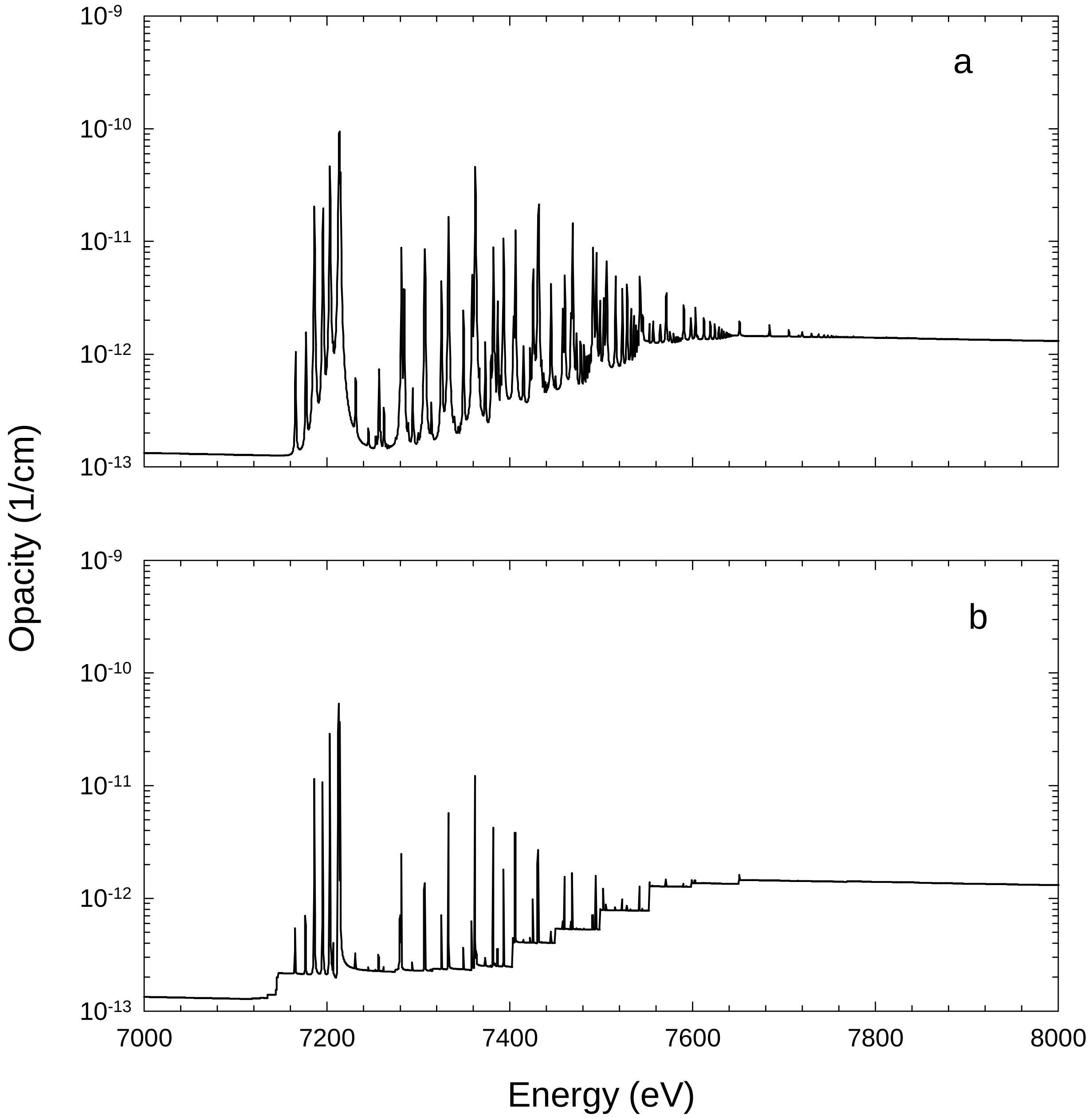

Fig. 3.— Opacities for a photoionized gas with solar elemental abundances and $\xi = 10$ including (a) K damped photoionization cross sections and (b) undamped cross sections.